DESIGNING WEAKLY COUPLED MEMS RESONATORS WITH MACHINE LEARNING-BASED METHOD

Fanping Sui†, Wei Yue†, Ruiqi Guo†, Kamyar Behrouzi, and Liwei Lin
Department of Mechanical Engineering, University of California, Berkeley, USA
†Fanping Sui, Wei Yue and Ruiqi Guo contributed equally to this work.

2022 IEEE 35th International Conference on Micro Electro Mechanical Systems Conference (MEMS) | 978-1-6654-0911-7/22/$31.00 ©2022 IEEE | DOI: 10.1109/MEMS51670.2022.9699450

ABSTRACT

We demonstrate a design scheme for weakly coupled resonators (WCRs) by integrating the supervised learning (SL) with the genetic algorithm (GA). In this work, three distinctive achievements have been accomplished: 1) the precise prediction of coupling characteristics of WCRs with an accuracy of 98.7% via SL; 2) the stepwise evolutionary optimization of WCR geometries while maintaining their geometric connectivity via GA; and 3) the highly efficient generation of WCR designs with a mean coupling factor down to 0.0056, which outperforms 98% of random designs. The coupling behavior analysis and prediction are validated with experimental data of coupled microcantilevers from a published work. As such, this newly proposed scheme could shed light upon the structural optimization methods for high-performance MEMS devices with high degree of design freedom.

KEYWORDS

Weakly Coupled Resonators, Machine Learning, Design Space Exploration

INTRODUCTION

The application of the mode localization phenomenon in the weakly coupled resonators (WCRs) has shown promising potential in the design and development of highly sensitive micro electrometers, force/strain sensors, and accelerometers [1]. In general, WCR designs with low coupling factors are desirable to achieve high sensing performance in the aforementioned applications [2]. While considerable efforts have been made towards developing high-performing WCRs, the physical understandings of the modal coupling behavior are still limited [3]. As such, it has been laborious to optimize the complex WCR systems with high degrees of design freedom based on human intuitions.

On the other hand, the emerging machine learning (ML) techniques have facilitated advancements in the field of microstructure designs [4, 5]. Most prior works have demonstrated that the underlying patterns for physical properties of MEMS structures, such as frequency characteristics and quality factors, can be captured and implicitly embedded in the deep neural networks by using the supervised learning (SL) algorithm. There is, however, a lack of well-defined inverse design strategies based on ML for the optimization of MEMS structures. Therefore, it is still very challenging to efficiently explore superior candidate designs in the high-dimensional design space, especially for the WCR design problems.

Intelligent searching algorithms, especially the genetic algorithm (GA), are proven to be excellent candidates for guiding the design space explorations [6, 7]. Inspired by the process of natural selection, GA is commonly adopted for decision-making problems with impressive performances. By transforming the 2D features of MEMS designs into the gene sequences, optimization for the desired properties can be conducted by biologically inspired numerical operations, such as selection, crossover, and mutation as shown in this work.

Here, we have developed a systematic approach for designing high-performance WCRs by the SL-GA scheme. The standard SL algorithm is utilized to capture the sophisticated mode coupling properties of WCRs via the deep neural networks. With sufficient training, the prediction accuracy of the SL-based model for the coupling factor of WCRs achieves a high score of 98.7%. The GA is integrated on top of this SL-based predictor for proposing progressively improved WCR design alternatives at each evolutionary iteration. By taking the advantage of the proposed SL-GA architecture, efficient exploration of high-performing WCR candidate designs in the astronomically large design space is demonstrated. As a result, the generated candidate designs can have a low mean coupling factor of 0.0056 from the proposed SL-GA framework and surpass ~98% of randomly generated designs.

SYSTEM ARCHITECTURE

The proposed SL-GA framework is illustrated by the flow chart in Figure 1. Each WCR design is represented by a 50×50 pixeled, black-and-white binary image, in which the black and white pixels correspond to solid constituent elements and empty spaces in the structure, respectively. The initial population of WCR designs is generated with two kinds of randomness introduced: 1) a random depth-first search (DFS) algorithm is applied for the formation of the prototype designs, and 2) some pixels are randomly added or removed from the prototype designs, giving rise to the initial designs. Such procedures ensure that the initial designs satisfy the geometric connectivity and promote the diversity of the topological features in the design populations for a wide range of coupling factors. Next, a customized deep residual neural network framework is adopted, featuring three main components: 1) convolutional layers for the 2D topological feature extraction; 2) residual blocks to enable the very deep networks and strong representation capabilities; and 3) fully connected layers for outputting coupling factor predictions. The neural network is pretrained in a supervised fashion and applied as a high-speed coupling behavior predictor with excellent accuracy.

The pixel-level 2D features of individual designs are encoded as the corresponding gene sequences to be applicable for the evolutionary processes. Among initial populations, designs with low predicted coupling factors are selected, forming the mating pool for subsequent crossover and random mutation steps. The crossover step is implemented by choosing two individual designs from

the mating pool as the elite parents, and randomly swapping the positions of structure pixels in the parent configurations for offspring generations. Subsequently, randomly selected newborns go through the mutation processes, which are applied by the random changes of the mutable genes in the design patterns. The porosity, defined as the ratio of the number of black pixels to the total number of pixels, is fixed in the design domain. To comply with this constraint, the mutation step is executed by adding and removing the same amounts of mutable genes at different locations. After the mutation process, the new generations could be formed with lower coupling factors than those of the previous generations. In this manner, the elite individuals representing designs with high performances are favored to survive and reproduce to result in progressively improved designs as the generation number increases. Examinations on the geometric connectivity are conducted in every step to define permissible operations, which prevents the formation of topological invalid designs. The selection, crossover and mutation steps constitute the whole procedure, which iterates until the desired coupling factor is achieved.

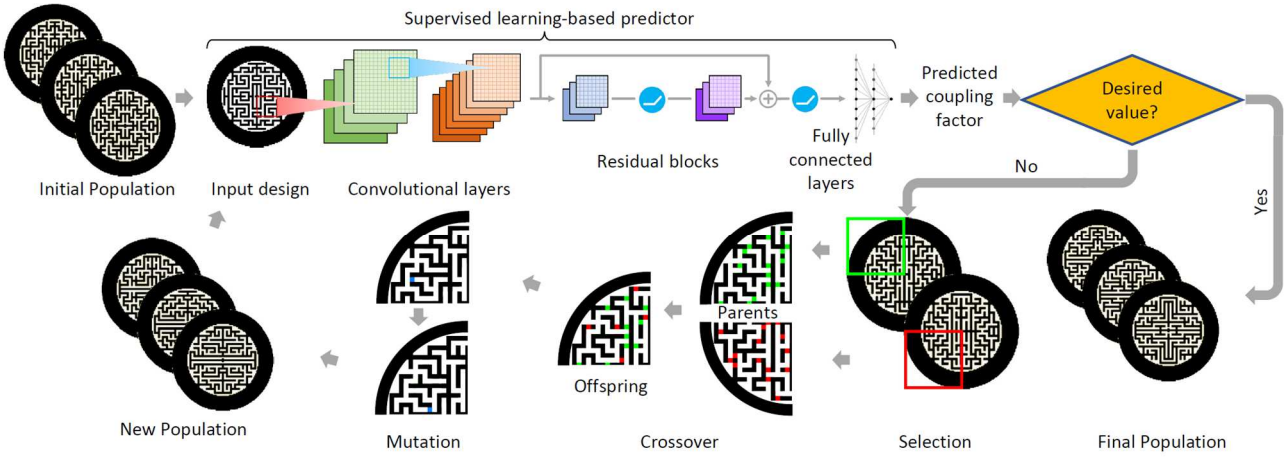

Figure 1: Overall flow chart of the proposed SL-GA framework. The framework consists of a customized deep residual neural network as an SL-based predictor, and a GA-based evolutionary procedure composed of the selection, crossover, and mutation steps. The green and red dots in the crossover section represent the exchangeable genes from the two parents. Similarly, the blue dots in the mutation section represent the mutable genes at the individual level. Such genes are defined to ensure the geometric connectivity. The iterative evolution stops when a desired value of coupling factor is reached in the generated design population.

MODE COUPLING IN DISK RESONATOR

The schematic of a circular-shaped disk resonator is demonstrated in Figure 2A. Polycrystalline silicon with Young's modulus, E = 150 GPa, density, ρ = 2.3 × 10^3 kg/m^3, and Poisson's ratio, v = 0.29 is used for the resonator modeling. The stem anchor is located at the center with a diameter of 1.76 μm and a thickness of 0.7 μm. The inner and outer diameters of the annular-shaped resonator structure are 30.8 μm and 44.0 μm, respectively. The geometries of the solid annular structure and stem anchor are fixed, which are linked by the adjustable labyrinth-like patterns. These patterns are initialized and updated with the designated porosity while satisfying the geometric connectivity criterion, which is defined as all the solid elements in the resonator body being linked together.

The mode coupling behavior of the disk resonators is investigated by analyzing their first two torsional modes. Since the geometry of a representative resonator in Figure 2A is symmetric, it has two symmetrical torsional modes with rotations along the X- and Y-directions as shown in Figure 2B(i). In order to create the mode coupling effects, we deliberately applied certain symmetry breaking features on the anchor of each design, resulting in the weakly coupled systems. After such modifications, the rotational axes of the new torsional modes are deflected as shown in Figure 2B(ii). This indicates the coupling phenomenon between the pure X- and Y-rotations, which is caused by the asymmetric constraint imposed on the anchor.

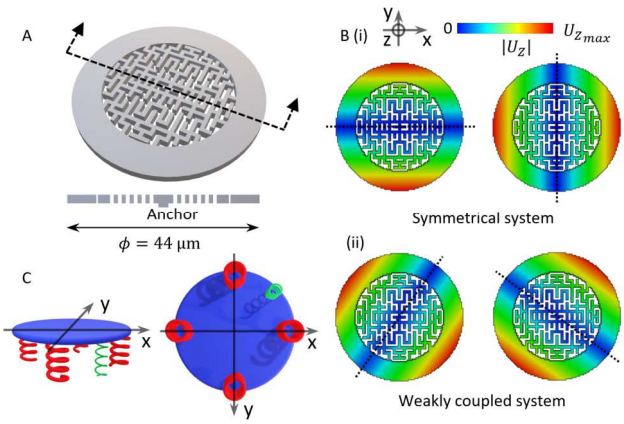

*Figure 2: **A**) Geometry of a representative disk-shaped resonator. **B**) Mode shapes of two torsional modes in (i) symmetrical systems, and (ii) weakly coupled systems. The asymmetrical system in **B**(ii) can be simplified by **C**) an equivalent vibrational disk model. Red springs represent the equivalent stiffness in the original symmetrical system while the green spring represents the equivalent coupling spring stiffness.*

The weakly coupled system with two torsional modes can be simplified to an equivalent model as shown in Figure 2C. The blue circular plate represents the resonator body, and the four red springs represent the elastic constraints imposed by the anchors and labyrinth-like

structures. The spring pairs placed on the X- and Y-axes account for the corresponding symmetrical torsional modes, respectively. The additional green spring, representing the asymmetric constraint, acts as a coupling spring to induce a weak coupling effect.

RESULTS AND DISCUSSION

Performances of SL-based predictor

Coupled microcantilevers from a previous work [8] have been utilized as a validation example for the proposed framework. By adjusting the geometric parameters, finite element analysis (FEA) simulations are implemented on similar but different microcantilevers. These results are used as the training dataset for the proposed SL-based predictor. The exact referenced structure is left out of the training dataset for performance evaluation. After using sufficient samples in the dataset for the training process, results from the SL-based predictor show exceptional agreements in terms of the coupling factor with structures both from the FEA simulations and experimental results as illustrated in Table 1. The small error of only 2.4% between the SL model and the experimental result illustrates the effectiveness of the proposed predictor and the feasibility of the approach. Furthermore, the coupling factor evaluated by FEA also matches well with the experimental data, with a relative error of 1.5%, which validates the simulation setups for the data generation scheme.

Table 1: Coupling factors of the coupled microcantilevers for validating the proposed SL-based predictor.

	Experimental Data [8]	FEA Simulation	SL-based Predictor
Coupling Factor	0.0328	0.0323	0.0320

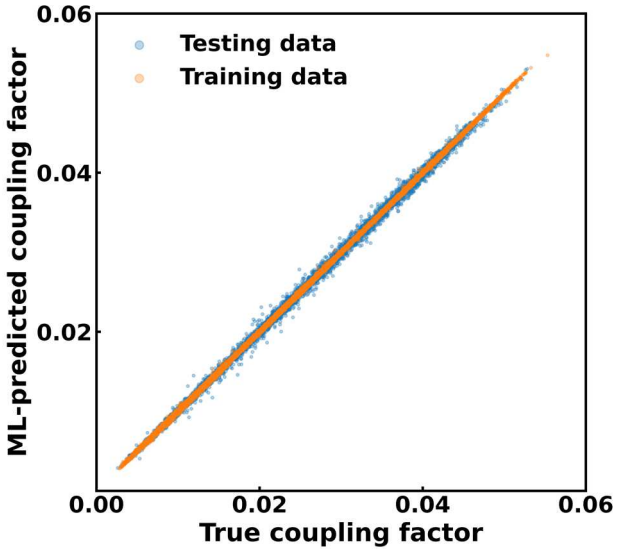

Figure 3: Predicted coupling factors given by the SL-based predictor compared with the simulated coupling factors acquired from FEA which are utilized as the true values.

For our weakly coupled disk-shaped micro resonators, the SL-based predictor is trained with computational results from over 100,000 FEA simulation tasks to accurately predict the coupling factors of individual designs. The accuracy of the SL-based predictor is analyzed before optimizing with the GA scheme. Figure 3 shows an excellent match with an accuracy of 98.7% between the predicted coupling factors by the SL model and the true coupling factors by FEA simulations. All the data points from both the training and testing datasets are located in a narrow band around the 45-degree line, implying the consistency between the predictions and the real values.

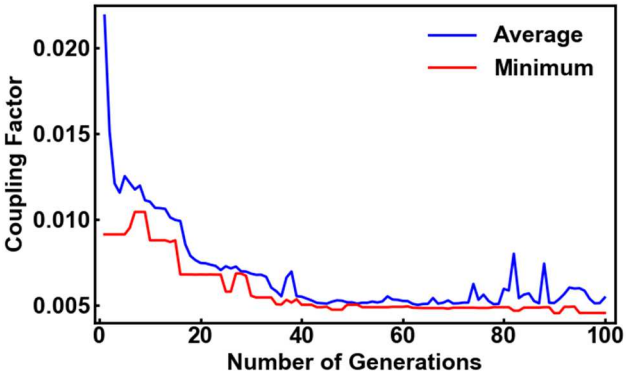

Figure 4: Averaged and minimum coupling factors with respect to the number of generations. As the number of generations increases, the curves drop steadily, indicating that the proposed candidate designs are progressively improved.

Optimization with GA

The learning curves in Figure 4 show the optimization process for the average and minimum coupling factors with respect to the number of generations, illustrating the effectiveness of the scheme. An initial population with the average and minimum coupling factors of 0.022 and 0.009, respectively, is chosen for the evolution iterations. In the first several generation cycles, well-performed individuals are selected and inferior ones are eliminated, resulting in the sharp decline of the curve. As the number of generation cycles increases, the influence of selection and mutation gradually fades and the change in the curve reduces. After 100 generations, the average and minimum coupling factor values decrease to 0.0054 and 0.0045, respectively. Finally, a high-ranking design with a minimum coupling factor of ~0.0027 is identified by the SL-GA framework after about 200 generations, which indicates an 88% reduction in coupling factor as compared to that from the initial designs.

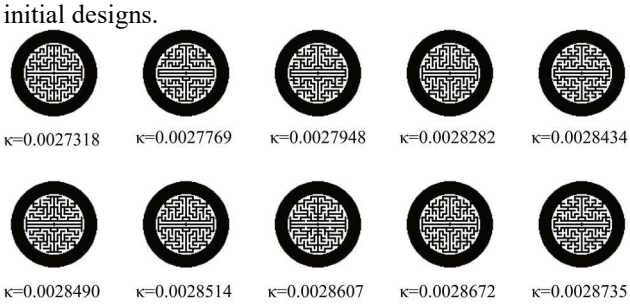

Figure 5: Geometric patterns with the smallest coupling factors generated by the proposed SL-GA framework.

The best 10 optimized candidate designs are listed in Figure 5, with some common beneficial features. For instance, a unidirectional beam in the middle is observed

among all the top designs, which is one key attribute for achieving such low coupling factors. This observation is intuitive since this key geometry feature can effectively intervene the influence from the torsional motions along the corresponding perpendicular directions, thus giving rise to the minimized coupling factors.

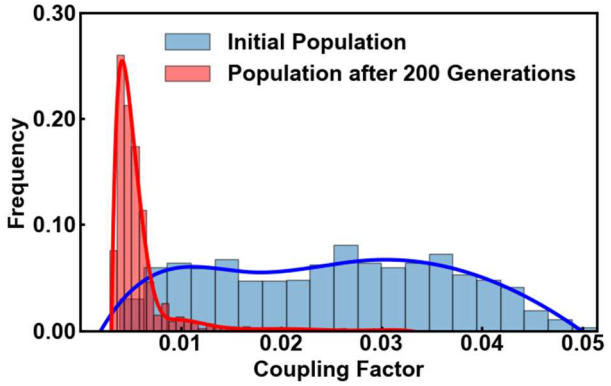

Figure 6: Coupling factor distributions of the initial random population and the final population after 200 generations. A significant distribution shift is observed, revealing the effective optimization consequence.

The distribution shift of the coupling factors is demonstrated in Figure 6, showing high efficiency of the proposed framework. Most initial designs have coupling factors in the wide range from 0.0035 to 0.05, with a relatively uniform distribution profile. After about 200 generations, final designs with significant performance enhancements are obtained. The resulting mean coupling factor can drop to 0.0056, outperforming ~98% of initial random designs. Furthermore, some elite individuals with coupling factors lower than 0.003 exist in the evolved populations, showing the capability of GA to search even better patterns out of the distribution of initial designs.

CONCLUSION

This paper demonstrates the optimization for MEMS WCR designs by machine learning-based method. A large amount of data generated from FEA is used to train the SL-based analyzer to predict coupling factors with good accuracy. Through the combination of the SL-based analyzer and the genetic algorithm, highly efficient evolutions are constructed to search the optimized resonator with the lowest coupling factor. It is found that within 200 generations, coupling factors are reduced significantly to reach a mean value of 0.0056 in the design population, which is lower than 98% of the initial random designs. Furthermore, the common features shared by the best designs are clearly observed as a design guideline for circular-shaped disk resonators with high sensitivity. As a future direction, we plan to implement more advanced intelligent design space exploration algorithms, such as Collaborative Deep Q-Networks and Conservative Q-Learning [9, 10], to optimize MEMS device designs with high computational efficiencies and improved performances.

ACKNOWLEDGEMENT

The authors appreciate the helpful discussion with Professor Grace X. Gu regarding this research.

REFERENCES

[1] A. Z. Hajjaj, N. Jaber, S. Ilyas, F. K. Alfosail, M. I. Younis, "Linear and Nonlinear Dynamics of Micro and Nano-Resonators: Review of Recent Advances", *Int. J. Non. Linear. Mech.*, vol. 119, p. 103328, 2020.

[2] H. Zhang, J. Huang, W. Yuan, H. Chang, "A High-Sensitivity Micromechanical Electrometer Based on Mode Localization of Two Degree-of-Freedom Weakly Coupled Resonators", *J. Microelectromechanical Syst.*, vol. 25, pp. 937–946, 2016.

[3] X. Zhou, C. Zhao, D. Xiao, J. Sun, G. Sobreviela, D. Gerrard, Y. Chen, I. Flader, T. Kenny, X. Wu, A. Seshia, "Dynamic modulation of modal coupling in microelectromechanical gyroscopic ring resonators", *Nat. Commun.*, vol. 10, p. 4980, 2019.

[4] R. Guo, R. Xu, Z. Wang, F. Sui, L. Lin, "Accelerating MEMS design process through machine learning from pixelated binary images", in *2021 IEEE 34th International Conference on Micro Electro Mechanical Systems (MEMS)*, Virtual, January 25–29, pp. 153–156, 2021.

[5] Q. Li, K. Lu, K. Wu, H. Zhang, X. Sun, X. Wu, D. Xiao, "A Novel High-Speed and High-Accuracy Mathematical Modeling Method of Complex MEMS Resonator Structures Based on the Multilayer Perceptron Neural Network", *Micromachines*, vol. 12, p. 1313, 2021.

[6] G. X. Gu, C. T. Chen, D. J. Richmond, M. J. Buehler, "Bioinspired hierarchical composite design using machine learning: Simulation, additive manufacturing, and experiment", *Mater. Horizons*, vol. 5, pp. 939–945, 2018.

[7] Y. Kim, Y. Kim, C. Yang, K. Park, G. X. Gu, S. Ryu, "Deep learning framework for material design space exploration using active transfer learning and data augmentation", *NPJ Comput. Mater.*, vol. 7, pp. 1–7, 2021.

[8] M. Spletzer, A. Raman, A. Q. Wu, X. Xu, R. Reifenberger, "Ultrasensitive mass sensing using mode localization in coupled microcantilevers", *Appl. Phys. Lett.*, vol. 88, p. 254102, 2006.

[9] F. Sui, R. Guo, Z. Zhang, G. X. Gu, L. Lin, "Deep Reinforcement Learning for Digital Materials Design", *ACS Mater. Lett.*, vol. 3, pp. 1433–1439, 2021.

[10] A. Kumar, A. Zhou, G. Tucker, S. Levine, "Conservative Q-Learning for Offline Reinforcement Learning", *arXiv preprint*, arXiv: 2006.04779, 2020.

CONTACT

*F. Sui; +1-510-993-5408; fpsui@berkeley.edu
*W. Yue; +1-510-984-8328; wei_yue@berkeley.edu